Supplementary Materials for

Role of Dissolved Oxygen in Metal(loid)s Removal by Zerovalent Iron at Different pH: Its Dependence on the Removal Mechanisms

Hejie Qin[a,b], Jinxiang Li[a], Qianqian Bao[a], Lina Li,[b] Xiaohong Guan[a,c] *

[a]State Key Laboratory of Pollution Control and Resources Reuse, College of Environmental Science and Engineering, Tongji University, Shanghai 200092, P. R. China

[b]Shanghai Synchrotron Radiation Facility, Shanghai Institute of Applied Physics, Chinese Academy of Sciences, Shanghai 201204, P. R. China

[c]Key Laboratory of Yangtze River Water Environment, Ministry of Education, College of Environment Science and Engineering, Tongji University, Shanghai 200092, China

*Author to whom correspondence should be addressed

Xiaohong Guan, email: guanxh@tongji.edu.cn; phone: +86-21-65980956

Number of pages (including this page): 9

Number of Figures: 5

Number of Tables: 1

Summary

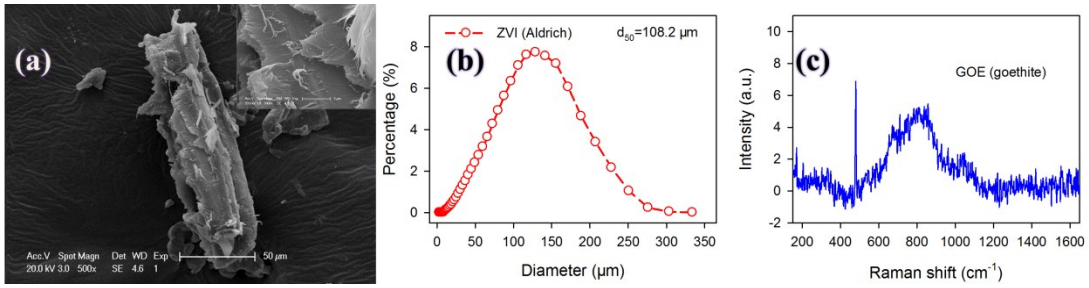

Figure S1. Basic properties of pristine ZVI used in this study, including morphological appearances, particle size and mineral on the surface. (a) The scanning electron microscopy image; (b) The particle size distribution; (c) The Raman spectra.

Morphological analysis was performed using a Hitachi 4700 microscope (at 15 kV). The size distribution of the Pri-ZVI particles was examined by Bettersize 2000 (Dandong Bettersize instruments Ltd., China). Raman spectra was collected using a DXR Raman Microscope (Thermo Fisher Scientific, Inc., China) with a 532 nm argon ion laser (2.0 mW), scanning from 100 cm^{-1} to 1700 cm^{-1} at room temperature. It should be noted that though the Raman spectroscopy identified FeOOH (goethite) in unreacted ZVI sample, it can be ignored for the very low quantity.

Table S1. Half reactions, the corresponding standard reduction potential, and conditional reduction potential for the redox species involved in this study.

Ox/Red	Half reaction	Standard reduction potential /V	Conditional reduction potential/V	
			pH 4.0	pH 6.0
Se(IV)/Se(0)	$HSeO_3^-+5H^++4e^- \rightarrow Se+3H_2O$	0.74	0.444	0.296
Cr(VI)/Cr(III)	$HCrO_4^-+7H^++3e^- \rightarrow Cr^{3+}+4H_2O$ (pH 4.0) $HCrO_4^-+4H^++3e^- \rightarrow Cr(OH)_3+H_2O$ (pH 6.0)	1.195	0.879	0.844
Cu(II)/Cu(0)	$Cu^{2+}+2e^- \rightarrow Cu$	0.34	0.34	0.34
Pb(II)/Pb(0)	$Pb^{2+}+2e^- \rightarrow Pb$	-0.127	-0.127	-0.127
O_2/O(-II)	$O_2+4H^++4e^- \rightarrow 2H_2O$	1.229	0.993	0.875
Fe(III)/Fe(II)	$Fe^{3+}+e^- \rightarrow Fe^{2+}$	0.769	0.769	0.769
Fe(II)/Fe(0)	$Fe^{2+}+2e^- \rightarrow Fe$	-0.44	-0.44	-0.44
$Fe(OH)_3/Fe^{2+}$	$Fe(OH)_3+e^- \rightarrow Fe^{2+}+3OH^-$	-1.51	0.26	-0.1

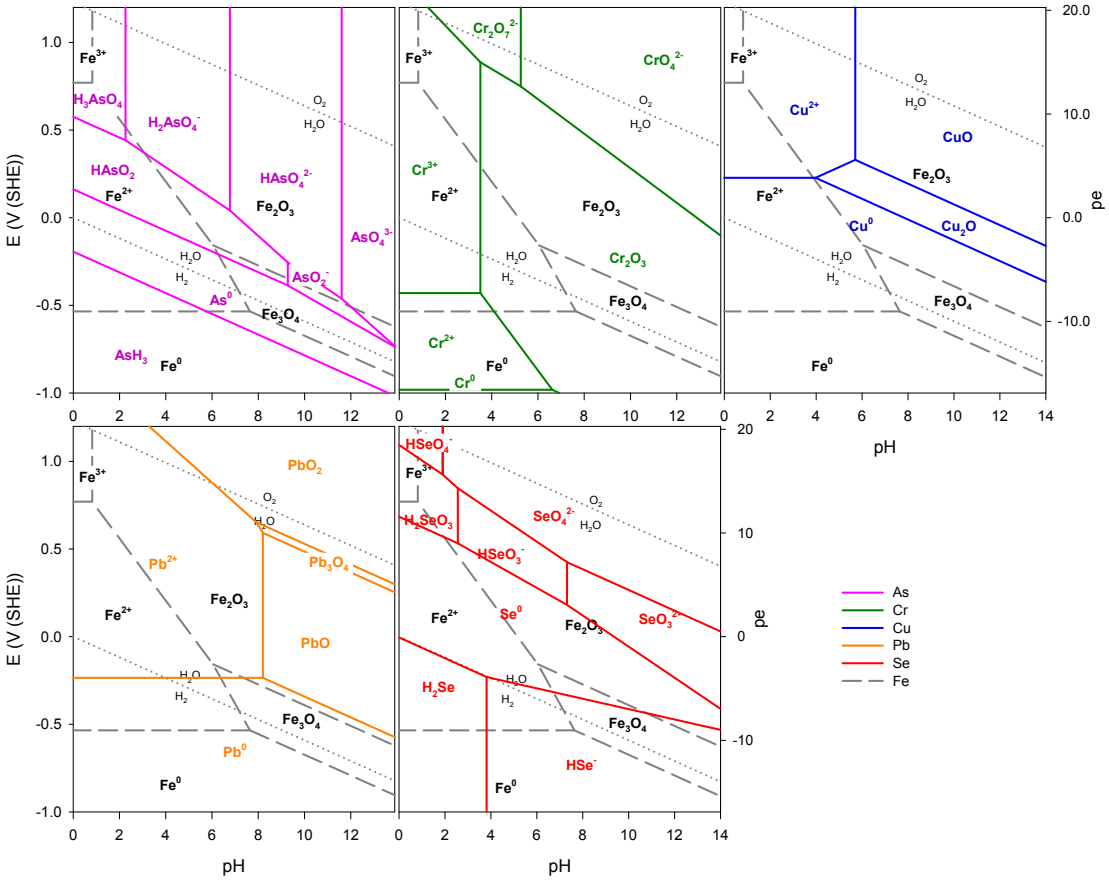

Figure S2. Eh–pH diagrams for species involved in this study (As(V) = 0.05 mM; Cr(VI) = 0.05 mM; Cu(II) = 0.2 mM; Pb(II) = 0.2 mM; Se(IV) = 0.2 mM; Temperature = 298 K; Suppressed iron phases: pyrite, pyrrhotite, and troilite.)

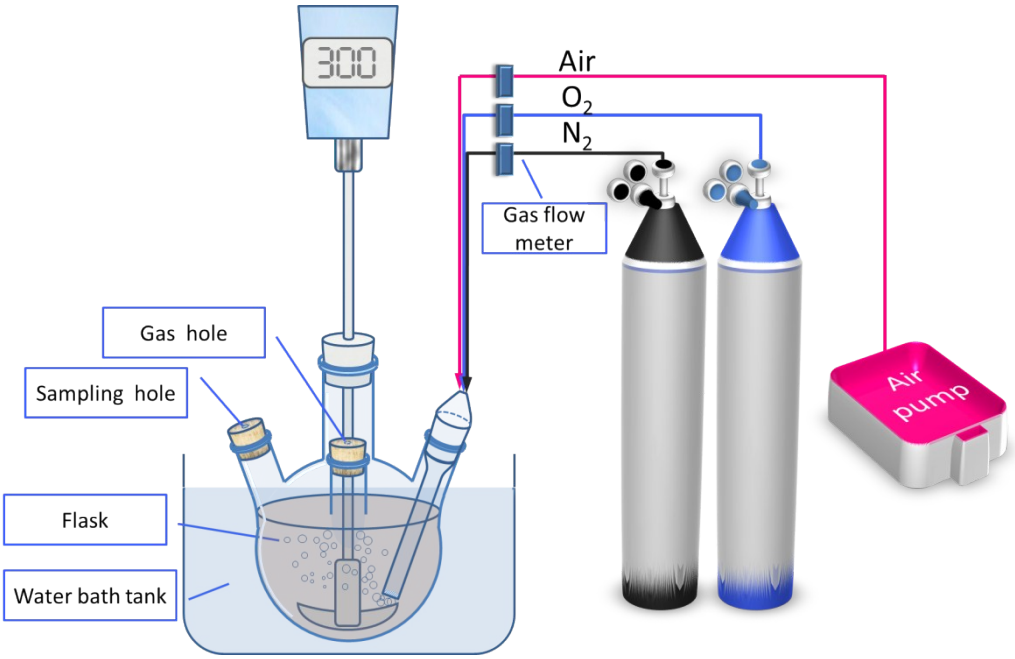

Figure S3. Schematic diagram of the experimental setup used in this study.

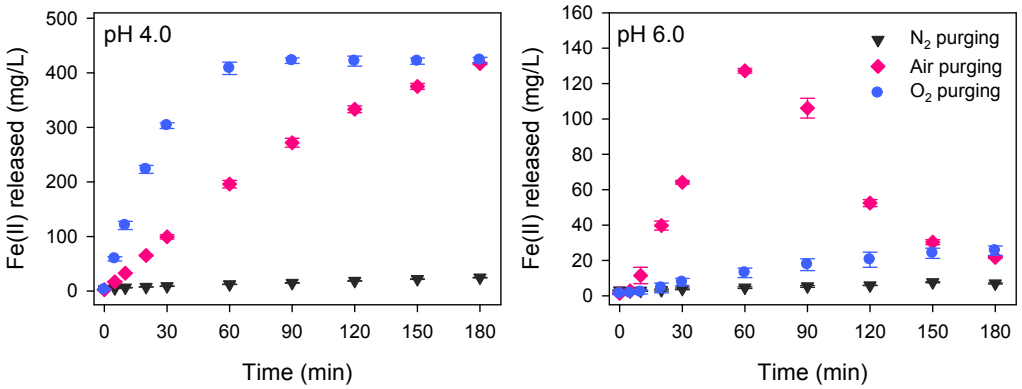

Figure S4. Kinetics of Fe(II) accumulation in the ZVI/H_2O systems without contaminant at pH 4.0 and 6.0. Reaction conditions: $[Fe^0]_0$ = 0.5 g/L, [NaCl] = 0.01 M.

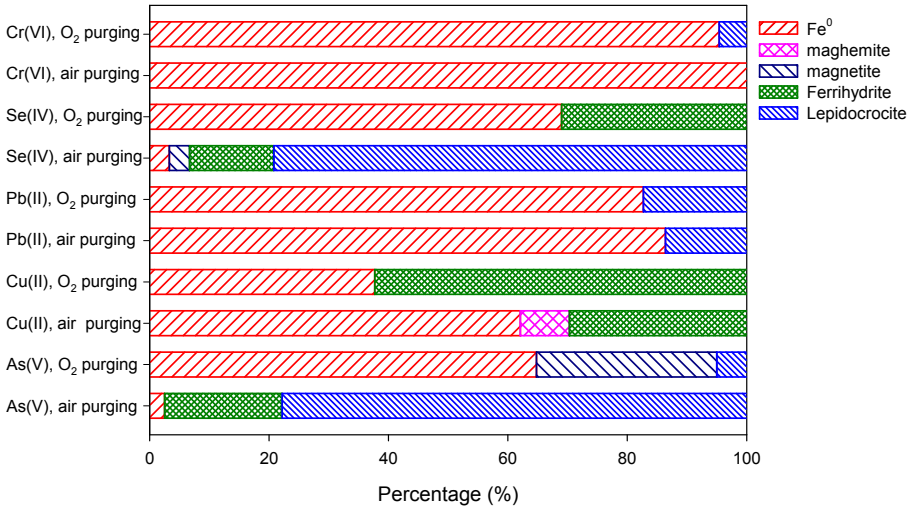

Figure S5. Fractions of different Fe species in reacted ZVI samples collected in the process of removal by ZVI at pH 6.0, which were derived from the LCF of Fe k^3-weighted EXAFS spectra (reaction time: 3 h).

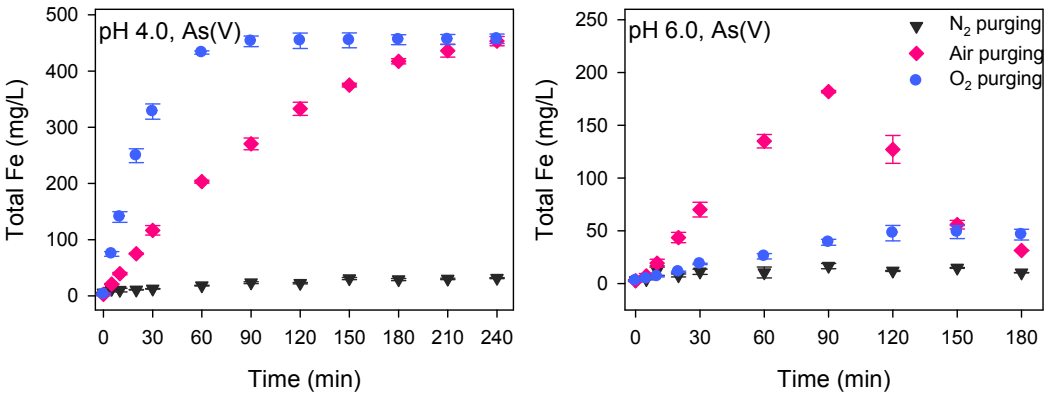

21

22 **Figure S6.** Concentration of total Fe in the ZVI/H_2O systems with As(V) at pH 4.0

23 and 6.0 (controlled).